Mechanics & Industry **18**, 106 (2017)

DOI: 10.1051/meca/2015115
www.mechanics-industry.org

Mechanics & Industry

Thermogravitational separation in horizontal annular porous cell

Oussama Abahri[1,a], Djamel Sadaoui[1], Kacem Mansouri[2], Abdelkader Mojtabi[3] and Marie Catherine Mojtabi[4]

[1] Laboratoire de Mécanique, Matériaux et Energétique (L2ME), Université Abderrahmane Mira de Béjaia, Campus de Targa Ouzemour, 06000 Béjaia, Algérie
[2] Laboratoire d'Energétique, Mécanique et Ingénieries (LEMI), Université M'Hamad Bougara, 3500 Boumerdès, Algérie
[3] IMFT, UMR CNRS/INP/UPS No. 5502, UFR MIG, Université Paul Sabatier, 118 route de Narbonne, 31062 Toulouse Cedex, France
[4] PHASE, EA 810, UFR PCA, Université Paul Sabatier, 118 routes de Narbonne, 31062 Toulouse Cedex, France

Received 19 August 2015, Accepted 26 November 2015

Abstract – Thermogravitational separation has until now, been used in different heated vertical cells called thermogravitational columns. The cell can be an annular cavity with two isothermal faces maintained at different temperatures. The main objective of this paper is to study the two dimensional coupled convection with thermodiffusion process. It concerns a theoretical and numerical investigation of species separation in a binary liquid mixture saturating a horizontal porous annulus space where the inner cylinder is heated isothermally. This kind of geometry is used instead of the annular vertical cell, hence the novelty of this technique. Analytical resolution is performed using the perturbation method function of time versus the corresponding physics (Raleigh and Lewis numbers...). Results reveal that the separation can be increased with an optimum for small values of Rayleigh number. Further, these values are less important than the critical value of Raleigh leading to the loss of unicellular flow stability found in literature.

Key words: Thermodiffusion / convection / perturbation method / porous medium

1 Introduction

Thermogravitational diffusion is the combination of two phenomena; convection and thermodiffusion. Coupling these two phenomena leads to species separation constituting a mixture of gas or liquid unfilled a well-defined geometrical space.

A literature survey related to this topic revealed that previous studies are substantially orientated toward the study of concave geometries and only few works deal with this type of geometry in the presence of porous media. Most of them are numerical studies. Clusius and Dickel [1] are among the first in the field: they have successfully carried out the separation of gas mixtures in a vertical cavity heated from one side (thermogravitational column, TGC). Soon thereafter Furry et al. [2] have developed a theoretical and experimental study on thermogravitation species separation in binary mixtures (FJO Theory) in order to interpret the experimental processes of isotope separation. Subsequently, many works appeared, in order to justify or extend the FJO theory and results on the binary liquid case [3]. Furthermore, other research on the improvement of experimental devices to increase separation can be found in literature. In this regard, Lorenz et al. [4] proposed the introduction of a porous medium into the cavity. Later, still regarding this topic, Caltagirone [5] used the perturbation method by developing the temperature and stream function in terms of Rayleigh number until order 3, to provide solution for low flow regimes. Thereafter, Burns and Yien [6] treated a steady flow with other types of boundary conditions for the inner cylinder (i.e. uniform temperature or imposed flow). They used the finite difference method for solving the linear system based on the S.O.R procedure and found the Caltagirone results for Dirichlet boundary conditions for the temperature. Later, Bau [7] investigated the effect of the cylindrical eccentricity on heat transfer, using a perturbation method with Rayleigh number as a development parameter. Indeed, Himasekhar [8] used the Galerkin method developed at higher levels to analyze the stability of two-dimensional unicellular flow with two different approaches. The first approach estimates the convergence of the obtained solution in terms of entire series of Rayleigh number, while the second one focuses on the linear stability of the obtained solution

[a] Corresponding author: oussama.abahri@gmail.com

Nomenclature

a^*	Thermal diffusivity of the mixture $a^* = \lambda^*/(\rho c)_f$
C	Mass fraction of the denser component of the mixture
D^*	Mass diffusion coefficient ($m^2.s^{-1}$)
D_T^*	Thermodiffusion coefficient ($m^2.s^{-1}.K^{-1}$)
e	Dimensional gap width $e = r_e - r_i$ (m)
$\mathbf{g}$	Gravitational acceleration ($m.s^2$)
k	Wave number
K	Permeability of the porous medium (m^2)
Le	Lewis number $Le = a^*/D^*$
P	Pressure of fluid (Pa)
R	Radius ratio $R = r_e/r_i$
Ra	Thermal filtration Rayleigh number $Ra = g\beta\,(T_i - T_e)\,(\rho c)_f K \;\; r_i/\lambda^*\nu$
Ra_c	Critical Rayleigh number
S	Separation
Sp	Separation factor
T	Temperature (K)
t	Dimensionless time
$\boldsymbol{V}$	Velocity field ($m.s^{-1}$)
V_φ, V_r	Velocity components ($m.s^{-1}$)
Greek symbol	
β_T	Thermal expansion coefficient (K^{-1})
β_C	Solutal expansion coefficient ($m^3.kg^1$)
ε	Porous medium porosity
$\acute{\varepsilon}$	Normalized porosity $\acute{\varepsilon} = \varepsilon/\sigma$
λ^*	Effective thermal conductivity of the porous medium mixture system ($W.m^{-1}.K^{-1}$)
$(\rho c)_f$	Volumetric heat capacity of the mixture ($J.m^{-3}.K^{-1}$)
$(\rho c)^*$	Effective volumetric heat capacity of porous medium mixture system ($J.m^{-3}.K^{-1}$)
ρ	Density
Subscripts	
e, i	Outer (external) and inner (internal)
o	Initial value
$*$	Equivalent thermophysical properties of the porous medium

for radius ratios ranging between $2^{1/8}$ and 2. Thus, they determine the critical Rayleigh numbers of transition between two-dimensional systems based on the radius ratio R. Dyko et al. [9] considered both linear and nonlinear stability of two-dimensional flow, using linear theory and the energy method. This study allows defining the criteria for the onset of the secondary flows observed experimentally. In fact, they obtained a critical Rayleigh number that delimited the flow stability from the linear stability analysis. Indeed, a subcritical Rayleigh number that defines a necessary condition for global flow stability was determined using the energy method. Therefore, Desrayaud et al. [10] consider thermogravitational separation of binary mixture and pure fluid in a horizontal annulus space delimited by two concentric and isothermal cylinders. They developed an analytical model able to describe the phenomenological equation of heat and mass transfer occurring in this space.

Also, Mojtabi et al. [11] obtained the following correlation for average Nusselt number in an annular space as a function of the Rayleigh number based on the layer thickness $\overline{Nu} = 1 + 17Ra\left(\left(r_e/r_i\right)^2 - \left(\left(r_e/r_i\right) - 1\right)^3\right)/40\,320$.

This correlation is still valid for an inner temperature higher than the outer one ($T_i > T_e$). It is sufficient to describe heat transfer inside the annular space for all values of Ra lower than 200. The difference compared with the numerical results is even smaller than the inner radius is less than $\sqrt{2}$. Under such conditions, an experimental visualization by Christiansen effect highlighted the existence ofunicellular and bi-cellular flows for different aspect ratios.

Recently works on the annular configuration, take into account changes in fluids properties (i.e. the Boussinesq assumption is no valid) thus the local thermal equilibrium between phases is not retained; $T_s \neq T_F$. Otherwise, preliminary studies concerning unicellular steady state flow characterized by a single convective cell in the annular layer was performed by [6]. More recently, Hadidi et al. [12] studied the double-diffusive free convective heat and mass transfer phenomena in a rectangular inclined cavity bounded by two adiabatic and impermeable horizontal walls and two isothermal vertical sides filled with two parallel porous layers. Results indicate that the permeability of the two porous layers has a significant effect

on the flow behavior and heat transfer. According to the numerical analysis three regimes has been distinguished; a diffusive regime for low values of R_K (permeability ratio), a transition regime where the mean Nusselt and Sherwood numbers increase with an increase of R_K and an asymptotic regime where Nu and Sh become independent of R_K.

Thorough analytical and numerical analysis conducted recently by Khouzam et al. [13] on species separation process in a binary fluid mixture within a horizontal rectangular cavity heated either from the top or the bottom, it was shown that the separation is controlled by horizontal temperature gradient and the upper moving wall. Further, in addition to five parameters setting the general problem, namely Ra, Pe, Pr, Le and ψ; the optimal separation solution is also influenced by the mass Peclet and Rayleigh numbers.

The present paper investigates analytically and numerically the separation of a binary mixture and pure fluid within a porous horizontal annulus. Both the inner and outer cylinders are heated isothermally, respectively T_i and T_o with $T_i > T_o$. In other words, we propose a new procedure coupling the convection and the thermodiffusion to obtain an important separation between the top and the bottom of the annular horizontal porous layer. This kind of geometry is used instead of the annular vertical cell and the classical rectangular one studied by Elhajjar et al. [14] or that of Oueslati et al. [15], hence the novelty of this technique.

2 Mathematical formulation

It should be recalled that thermodiffusion effect induces a mass fraction gradient in binary fluid mixtures subjected to a temperature gradient. In addition to the usual isothermal contribution, there is an additional contribution proportional to the concentration, so that:

$$\vec{J} = -\rho\ D\ \nabla\ C - \rho C\,(1-C)\,D_T\ \nabla T \tag{1}$$

where D is the mass diffusion coefficient, D_T the thermodiffusion coefficient, ρ the density, and C the mass fraction of the denser component.

The investigated problem is illustrated schematically in Figure 1, which consists of an annular porous layer between two coaxial horizontal cylinders of length L. The inner cylinder of radius r_i is at fixed warm temperature T_i while the outer cylinder of radius r_e is maintained at constant and uniform temperature T_e with $T_e < T_i$.

Darcy's law is assumed valid where fluid and solid phases are in local thermal equilibrium. It is also assumed that viscous dissipation, compressibility and Dufour effects are neglected [14] because of their minor influence on liquid mixture. Also, the Boussinesq approximation is invoked for binary fluid properties to relate the density changes to temperature and concentration and to couple in this way the temperature and concentration fields to the flow field:

$$\rho = \rho_0\ [1 - \beta_T\,(T - T_0) - \beta_C\,(C - C_0)] \tag{2}$$

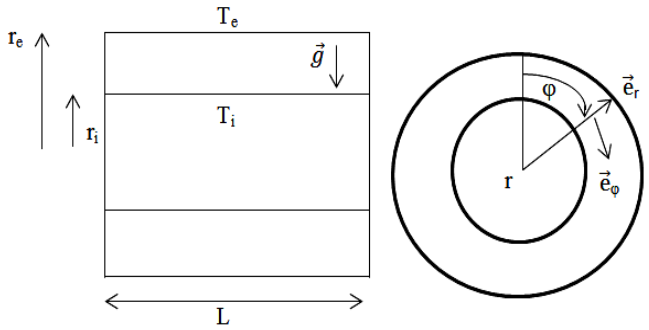

Fig. 1. Geometry of the physical problem.

Here, β_T and β_c are the coefficients of thermal and solutal expansion, respectively, while ρ_0 is the fluid mixture reference density at temperature T_0 and mass fraction c_0.

Under these assumptions, the equations of continuity, momentum, energy and chemical species are cast in their dimensional form as follow:

$$\begin{cases} \nabla \cdot (\boldsymbol{V}) = 0 \\ \boldsymbol{V} = -\frac{K}{\mu}\,(\nabla P - \rho \boldsymbol{g}) \\ \lambda^* \nabla^2 T\ = (\rho c)^*\,\frac{\partial T}{\partial t} + \ (\rho c)_f\,\boldsymbol{V}\cdot\nabla T \\ \varepsilon \frac{\partial C}{\partial t} + \boldsymbol{V}\cdot\nabla C = D^*\nabla^2 C + D_T^* C_0\,(1-C_0)\,\nabla^2 T \end{cases} \tag{3}$$

Here it was assumed that there is little variation in the term $C\,(1-C)$ of the species equation, so that it can be replaced by $C_0\,(1-C_0)$; with C_0 the initial mass fraction.

Equations (3) were transformed in the non-dimensionalized form by scaling length, time and temperature by r_i; $\left[(\rho c)^* r_i^2/\lambda^*\right]$ and $[T_i - T_e]$, and the velocity, pressure and mass fraction by $[\lambda^*/(r_i(\rho c)_f)]$; $[\lambda^*\mu/(k(\rho c)_f)]$ and $\Delta C = -\Delta T c_0(1-c_0)D_T^*/D^*$, respectively.

Thus, the dimensionless governing conservation equations for mass, momentum, energy and chemical species are:

$$\begin{cases} \nabla \cdot (\boldsymbol{V}) = 0 \\ \boldsymbol{V} = Ra\,(T + sp C)\,\boldsymbol{e_z} \\ \frac{\partial T}{\partial t} + \boldsymbol{V}\cdot\nabla T = \nabla^2 T \\ \varepsilon' \frac{\partial C}{\partial t} + \boldsymbol{V}\ \cdot\nabla C = \frac{1}{Le}(\nabla^2 C - \nabla^2 T) \end{cases} \tag{4}$$

The studied problem depends on five non-dimensional parameters; the thermal filtration Rayleigh number $Ra = g\beta\,(T_i - T_e)\,(\rho c)_f K\quad r_i/\lambda^*\nu$; the Lewis number $Le = a^*/D^*$; the normalized porosity $\acute{\varepsilon} = \varepsilon/\sigma$; the separation ratio $sp = -\ (\beta_C/\beta_T)\,(D_T^*/D^*)\,C_0\,(1-C_0)$ and the aspect ratio $R = r_e/r_i$.

Here $\sigma = (\rho c)^*/(\rho c)_f$ where $(\rho c)^*$ is the effective volumetric heat capacity of the porous medium, and a^* the effective thermal diffusivity of the porous medium.

Using polar coordinates (r, φ) and the associated local database (e_r, e_φ), the velocity can be defined by:

$$\boldsymbol{V} = V_r \boldsymbol{e_r} + V_\varphi \boldsymbol{e_\varphi} \tag{5}$$

The vector e_Z takes the following form: $\boldsymbol{e_z} = \cos(\varphi)\,\boldsymbol{e_r} - \sin(\varphi)\boldsymbol{e_\varphi}$.

With V_r and V_φ are the radial and tangential velocity component, respectively.

Using stream function formalism, the velocity components can be expressed as:

$$V_r = \frac{1}{r}\frac{\partial \psi}{\partial \varphi} \quad \text{and} \quad V_\varphi = -\frac{\partial \psi}{\partial r}$$

The continuity equation is identically satisfied, by taking the rotational of Darcy's equation. Studying the steady state we have to solve the following system:

$$\begin{cases} \nabla^2\psi = Ra\left[\sin(\varphi)\,\dfrac{\partial}{\partial r}\,(T + sp\;C) \right. \\ \qquad \left. + \dfrac{\cos(\varphi)}{r}\dfrac{\partial}{\partial \varphi}\,(T + sp\;C\;)\right] \\ \nabla^2 T = \dfrac{1}{r}\;\left[\dfrac{\partial \psi}{\partial \varphi}\;\;\dfrac{\partial T}{\partial r} - \dfrac{\partial \psi}{\partial r}\;\;\dfrac{\partial T}{\partial \varphi}\right] \\ \nabla^2 C - \nabla^2 T = \dfrac{Le}{r}\left[\dfrac{\partial \psi}{\partial \varphi}\;\dfrac{\partial C}{\partial r} - \dfrac{\partial \psi}{\partial r}\dfrac{\partial C}{\partial \varphi}\right] \\ \nabla^2 . = \dfrac{\partial^2 .}{\partial r^2} + \dfrac{1}{r}\dfrac{\partial .}{\partial r} + \dfrac{\partial^2 .}{r^2 \partial \varphi^2} \end{cases} \tag{6}$$

The corresponding dimensionless boundary conditions are:

$$\begin{cases} T = 1 \quad \text{for} \quad r = 1, \qquad \psi = \dfrac{\partial^2 \psi}{\partial r^2} = 0,\; \dfrac{\partial C}{\partial r} = \dfrac{\partial T}{\partial r}, \\ \qquad\qquad \forall \varphi \in [0, 2\pi] \\ T = 0 \quad \text{for} \quad r = R, \;\; \psi = \dfrac{\partial^2 \psi}{\partial r^2} = 0, \dfrac{\partial C}{\partial r} = \dfrac{\partial T}{\partial r}, \\ \qquad\qquad \forall \varphi \in [0, 2\pi] \\ \varphi = 0, \pi \quad \dfrac{\partial T}{\partial \varphi} = \dfrac{\partial C}{\partial \varphi} = 0, \qquad \psi = 0, \qquad \forall r \end{cases} \tag{7}$$

For symmetric regime and single-cell system r varies in the range [1–R], with $R = r_e/r_i$. Moreover, a new variable can be introduced in function of temperature and the concentration $\eta = C - T$.Thus, the coupled system takes the form:

$$\nabla^2\psi = Ra\left[\sin(\varphi)\,\frac{\partial}{\partial r}\,((1+sp)\,T + sp\;\eta) + \frac{\cos(\varphi)}{r}\frac{\partial}{\partial \varphi}\,((1+sp)T + sp\;\eta\;)\right] \tag{8}$$

$$\nabla^2 T = \frac{1}{r}\;\left[\frac{\partial \psi}{\partial \varphi}\;\;\frac{\partial T}{\partial r} - \frac{\partial \psi}{\partial r}\;\;\frac{\partial T}{\partial \varphi}\right] \tag{9}$$

$$\nabla^2 \eta = \frac{Le}{r}\left[\frac{\partial \psi}{\partial \varphi}\;\frac{\partial}{\partial r}\,(T+\eta) - \frac{\partial \psi}{\partial r}\frac{\partial}{\partial \varphi}(T+\eta)\right] \tag{10}$$

3 Results and discussion

3.1 Analytical results

An analytical resolution, of the coupled mass, energy and momentum equations (Eqs. (8) to (10)) using the perturbation method is conducted in this section. The development is performed till second order.

Perturbation method is an approximation technique based on the principle of asymptotic expansion; the proposed solution is generally represented by the first developed terms. This development may involve a parameter (large or small) that appears in the equations, or that artificially introduced. It is called disturbance parameter.

In the present study, this method leads to express temperature, stream function and concentration as an expansion of Rayleigh number:

$$\begin{aligned} \psi &= \sum_{i=1}^{n} Ra^i\,\psi_i(r,\varphi) \\ T &= \sum_{i=0}^{n} Ra^i\,T_i(r,\varphi) \\ \eta &= \sum_{i=0}^{n} Ra^i\,\eta_i(r,\varphi) \end{aligned} \tag{11}$$

By introducing these three expressions in Equations (8) to (10), we obtain an infinite sequence of coupled partial differential equations that can be solved analytically by recurrence.

The zero order is given by:

$$\nabla^2 T_0 = 0 \tag{12}$$

$$\nabla^2 \eta_0 = 0 \tag{13}$$

The following equation system is resulting from the development at order 1:

$$\nabla^2\psi_1 = \sin(\varphi)\left[(1+sp)\,\frac{\partial T_0}{\partial r} + sp\frac{\partial \eta_0}{\partial r}\right] + \frac{\cos(\varphi)}{r}\left[(1+sp)\,\frac{\partial T_0}{\partial \varphi} + sp\frac{\partial \eta_0}{\partial \varphi}\right] \tag{14}$$

$$\nabla^2 T_1 = \frac{1}{r}\;\left[\frac{\partial \psi_1}{\partial \varphi}\;\;\frac{\partial T_0}{\partial r} - \frac{\partial \psi_1}{\partial r}\;\;\frac{\partial T_0}{\partial \varphi}\right] \tag{15}$$

$$\nabla^2 \eta_1 = \frac{Le}{r}\left[\frac{\partial \psi_1}{\partial \varphi}\;\frac{\partial}{\partial r}\,(T_0+\eta_0) - \frac{\partial \psi_1}{\partial r}\frac{\partial}{\partial \varphi}(T_0+\eta_0)\right] \tag{16}$$

The system developed at order 2 is given by:

$$\nabla^2\psi_2 = \sin(\varphi)\left[(1+sp)\,\frac{\partial T_1}{\partial r} + sp\frac{\partial \eta_1}{\partial r}\right] + \frac{\cos(\varphi)}{r}\left[(1+sp)\,\frac{\partial T_1}{\partial \varphi} + sp\frac{\partial \eta_1}{\partial \varphi}\right] \tag{17}$$

$$\nabla^2 T_2 = \frac{1}{r}\;\left[\frac{\partial \psi_2}{\partial \varphi}\;\;\frac{\partial T_0}{\partial r} + \;\;\frac{\partial \psi_1}{\partial \varphi}\frac{\partial T_1}{\partial r} - \frac{\partial \psi_2}{\partial r}\;\;\frac{\partial T_0}{\partial \varphi} - \frac{\partial \psi_1}{\partial r}\frac{\partial T_1}{\partial \varphi}\right] \tag{18}$$

$$\nabla^2\eta_2 = \frac{Le}{r}\left[\begin{array}{l}\dfrac{\partial\psi_1}{\partial\varphi}\ \dfrac{\partial}{\partial r}\left(T_1+\eta_1\right)+\dfrac{\partial\psi_2}{\partial\varphi}\ \dfrac{\partial}{\partial r}\left(T_0+\eta_0\right)\\ -\dfrac{\partial\psi_1}{\partial r}\ \dfrac{\partial}{\partial\varphi}\left(T_1+\eta_1\right)\\ -\left(\dfrac{\partial\psi_2}{\partial r}\ \dfrac{\partial}{\partial\varphi}\left(T_0+\eta_0\right)\right)\end{array}\right] \tag{19}$$

At order N the equations that can be solved analytically take the following general form:

$$\left\{\begin{array}{l}\nabla^2\psi_{(i)} = \sin(\varphi)\left[(1+sp)\dfrac{\partial T_{(i-1)}}{\partial r}+sp\dfrac{\partial\eta_{(i-1)}}{\partial r}\right]\\ +\dfrac{\cos(\varphi)}{r}\left[(1+sp)\dfrac{\partial T_{(i-1)}}{\partial\varphi}+sp\dfrac{\partial\eta_{(i-1)}}{\partial\varphi}\right]\\ \nabla^2 T_{(i)} = \displaystyle\sum_{j=1}^{n}\frac{1}{r}\left[\frac{\partial\psi_j}{\partial\varphi}\ \frac{\partial T_{(i-j)}}{\partial r}-\frac{\partial\psi_j}{\partial r}\ \frac{\partial T_{(i-j)}}{\partial\varphi}\right]\\ \nabla^2\eta_{(i)} = \displaystyle\sum_{j=1}^{n}\frac{Le}{r}\left[\frac{\partial\psi_j}{\partial\varphi}\ \frac{\partial}{\partial r}\left(T_{(i-j)}+\eta_{(i-j)}\right)\right.\\ \left.-\dfrac{\partial\psi_j}{\partial r}\dfrac{\partial}{\partial\varphi}(T_{(i-j)}+\eta_{(i-j)})\right]\end{array}\right. \tag{20}$$

The associated boundary conditions are:

$T_0 = 0$ for $r = 1$ $\frac{\partial\eta}{\partial r} = 0$, $\psi_{(i)} = 0$, for $r = 1, R$ for any value of i.
$T_0 = 0$ for $r = R$, $\frac{\partial\eta}{\partial\varphi} = \frac{\partial T}{\partial\varphi} = 0, \psi_{(i)} = 0$ for $\varphi = 0, \pi$ for any value of i.
$T_{(i)} = 0$ for $r = 1, R,\ i \geqslant 1$.

Taking into account the boundary conditions of temperature and concentration and after direct integration, the following expressions are obtained for zero order:

$$T_0 = 1 - \frac{\ln(r)}{\ln(R)} \tag{21}$$

$$\eta_0 = \text{cte} \tag{22}$$

By recurrence and after replacing T_0 and η_0 by their expressions in Equation (14) the following partial differential equation is obtained:

$$\frac{\partial^2\psi_1(r,\varphi)}{\partial r^2}+\frac{1}{r}\frac{\partial\psi_1}{\partial r}+\frac{1}{r^2}\frac{\partial^2\psi_1(r,\varphi)}{\partial\varphi^2} + \frac{(1+sp)}{r\ln(R)}\sin(\varphi) = 0 \tag{23}$$

Using the separation of variables method, the solution at order 1 of Equation (23) is:

$$\psi_1 = \left(\begin{array}{c}\dfrac{1}{4}\dfrac{r\,(1+sp)\,(2R^2\ln(R)-R^2+1)}{\ln(R)\,(R^2-1)}\\ -\dfrac{R^2\,(1+sp)}{2r\,(R^2-1)}-\\ \dfrac{r\,(2\ln(R)-1)\,(1+sp)}{4\ln(R)}\end{array}\right)\sin(\varphi) \tag{24}$$

The same procedure is applied to the temperature where the following equation should be solved:

$$\frac{\partial^2 T_1(r,\varphi)}{\partial r^2}+\frac{1}{r}\frac{\partial T_1}{\partial r}+\frac{1}{r^2}\frac{\partial^2 T_1(r,\varphi)}{\partial\varphi^2}\ +Q(r)\cos(\varphi) = 0 \tag{25}$$

with,

$$Q(r) = \frac{1}{r^2\ln(R)}\left(\begin{array}{c}\dfrac{r\,(1+sp)\,(2R^2\ln(R)-R^2+1)}{4\ln(R)\,(R^2-1)}\\ -\dfrac{R^2(1+sp)}{2\ r(R^2-1)}-\\ \dfrac{r\,(2\ln(r)-1)\,(1+sp)}{4\ \ln(R)}\end{array}\right) \tag{26}$$

In this case, the corresponding solution of Equation (25) takes the following form:

$$T_1 = \left(a_1 r\ln^2(r)+a_2 r\ln(\ r)+a_3 r^{-1}\ln(r) +a_4 r^{-1}+a_5 r\right)\cos(\varphi) \tag{27}$$

where, a_i are coefficients that depend only on the ratio R and the separation factor sp.

Similarly η takes the form partial differential equation form as the temperature:

$$\frac{\partial^2\eta_1(r,\varphi)}{\partial r^2}+\frac{1}{r}\frac{\partial\eta_1}{\partial r}+\frac{1}{r^2}\frac{\partial^2\eta_1(r,\varphi)}{\partial\varphi^2}+g(r)\cos(\varphi) = 0 \tag{28}$$

with,

$$g(r) = \frac{Le}{r^2\ln(R)}\left(\begin{array}{c}\dfrac{r\,(1+sp)\,(2R^2\ln(R)-R^2+1)}{4\ln(R)\,(R^2-1)}\\ -\dfrac{R^2(1+sp)}{2\ r(R^2-1)}-\\ \dfrac{r\,(2\ln(r)-1)\,(1+sp)}{4\ \ln(R)}\end{array}\right) \tag{29}$$

Then, the solution of this equation is:

$$\eta_1 = Le\left(b_1 r+b_2 r^{-1}+b_3 r^{-1}\ln(r)+b_4 r\ln(r) +b_5 r\ln(r)^2\right).\cos(\varphi) \tag{30}$$

where, b_i are coefficients that depend only on the ratio R and the factor sp.

Further, the concentration $c_{(i)}$ are identified using the relationship between:

$$c_{(i)} = \eta_{(i)} + T_{(i)} \tag{31}$$

After injecting the temperature, the concentration and the current function found previously at order 1 and order in Equation (17), and after using the separation variables method, the current function at order 2 (ψ_2) takes the following form:

$$\psi_2 = \left(c_1 r^2 ln^2(r)+c_2 r^2 ln(\ r)+c_3 ln(r)+c_4 r^2 +c_5+c_6 r^{-2}\right)\ \sin(2\varphi) \tag{32}$$

Concerning the temperature at order 2, this variable assumes the general following form:

$$T_2 = f_T(r)\cos(2\varphi) + g_T(r) \tag{33}$$

And also for the concentration:

$$\eta_2 = f_\eta(r)\cos(2\varphi) + g_\eta(r) \tag{34}$$

where c_i, $f_T(r)$, $f_\eta(r)$, $g_T(r)$, and $g_\eta(r)$ are function of R and the separation factor

Expressions of temperature, stream function and concentration at a given point will be approximated by the three equations developed earlier:

$$\begin{cases} \psi = Ra\psi_1 + Ra^2\psi_2 \\ T = T_0 + RaT_1 + Ra^2T_2 \\ \eta = \eta_0 + Ra\eta_1 + Ra^2\eta_2 \end{cases} \tag{35}$$

Here, the perturbation method is applicable only for small values of Rayleigh number.

3.2 Numerical results

To highlight the developed analytical method, analytical results are compared against those obtained by solving the basic equations of the coupled model. It is undertaken using COMSOL Multiphysics code [16] which is a powerful environment for modeling and solving a variety of research and engineering problems based on the finite element method (FE). Moreover, this software is particularly adapted for the treatment of Multiphysical problems where several phenomena are simultaneously studied. Thus, the assessment of the incidence of heat and mass transfer on other phenomena such as the ingress of aggressive agents (chlorides, ions) and the ingress of pollutants (Volatile Organic Compounds) becomes possible. Also, different kind of meshes are easily generated which is more convenient for 3D studies. It is obvious that the accuracy of numerical results is function of the mesh size.

To find a proper grid size, a grid testing is performed using various grid combinations (90×10 to 180×20) of control volumes. For each grid size, separation (S) and Nusselt number (Nu) are presented in Figure 2 for $Ra = 10$, $sp = 0.1$, $R = 35/32$ and $Le = 100$. Throughout this investigation, grid sizes greater or equal than 150×20 are sufficient to have a solution independent of the mesh. Hence, considering both the accuracy and the computational costs, most computations reported in the current work were performed with a multiple grid system of 150×20, leading to good agreement between the numerical and analytical results.

Figure 3 represents the isoconcentration lines within an annular space of aspect ratio $r = 35/32$, obtained for different Ra (0.1, 10 and 100, respectively). In order to highlight the effect of Ra alone, both Lewis number, R and sp were kept constant at values. As seen, the form of the isoconcentration line is affected by the increasing value of Ra. Increasing the Rayleigh number intensifies

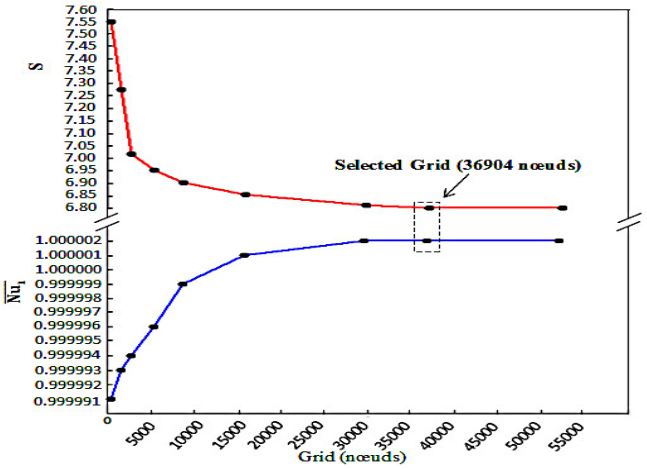

Fig. 2. Detail of the grid dependency.

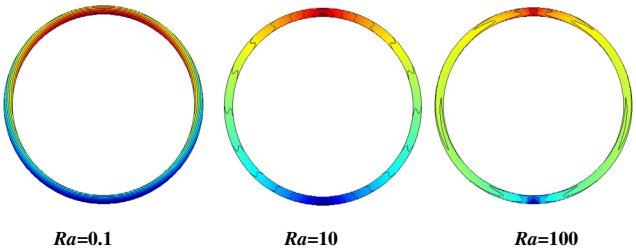

Fig. 3. Iso-concentration for $Le = 100$, $sp = 0.1$ and $R = 35/32$ for $Ra = 0.1$, $Ra = 10$ and $Ra = 100$ from the left to the right side.

distortions of the concentration profiles, particularly in the vicinity of the two poles. In fact, for a low value of Ra (0.1), it can be seen that these isoconcentrations have quasi-uniform and homogeneous radial distribution along the horizontal cell. This means that the separation is mainly due to the thermodiffusion where the role of the convection is almost negligible. When increasing Ra, convection velocity rises; this affects the isoconcentrations curvatures; so that concentration plumes emerge above the poles of the inner cylinder, which signal an increase in the mass transfer rate, as is indicated in Figure 3b. Therefore, we approach increasingly from horizontal separation, in which case the coupling convection/ thermodiffusion is optimal. For $Ra = 100$, the convection develops compared to the thermodiffusion, this promotes instability of the isoconcentrations repartition and therefore the separation decreases significantly.

4 Comparison between analytical and numerical results

In this section, we compared results of a numerical solution obtained by the finite element method (COMSOL) to those given by an analytical method developed above. The analytical method used to solve the coupled Equations (8)–(10) with the associated boundary

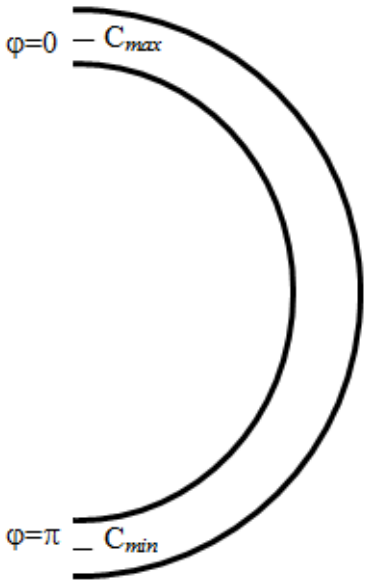

Fig. 4. Separation concept.

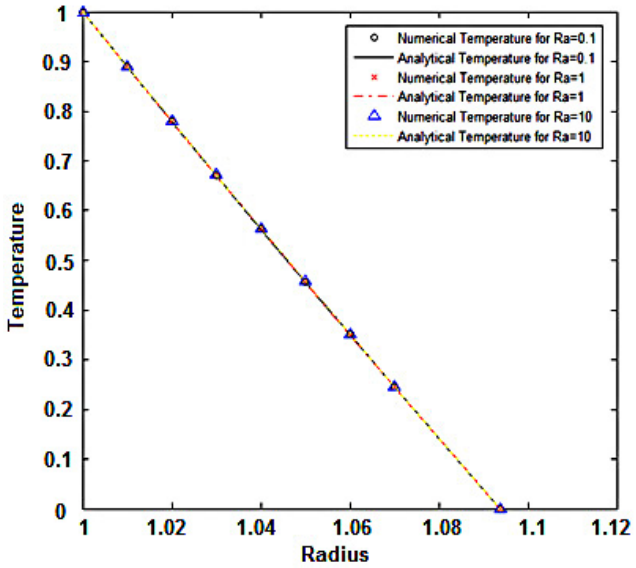

Fig. 5. Analytical and numerical temperature for different Ra and for $Le = 100$, $sp = 0.1$, $\phi = 0$ and $R = 35/32$.

conditions (7) is a perturbation technique based on the principle of asymptotic expansion with a development till second order. The developed perturbation method is applicable only for low Rayleigh numbers.

The comparison is based on the main variables of the problem; namely the stream function (ψ); temperature (T), mean Nusselt number (Nu) and separation (S). The global Nusselt number characterizing the rate of total heat transfer is defined as the ratio of the total heat flux to the conductive heat flux through the same surface. Thus, the internal and external Nusselt can be defined as follow:

$$Nu_{gi} = -\frac{\ln(R)}{\pi}\int_0^{\pi}\left[\frac{\partial T}{\partial r}\right]_{r=1} \mathrm{d}\varphi$$

$$Nu_{ge} = -R\frac{\ln(R)}{\pi}\int_0^{\pi}\left[\frac{\partial T}{\partial r}\right]_{r=R} \mathrm{d}\varphi$$

The separation factor (S) is defined as the difference of the mass fractions of the heavier component between two points $[(R+1)/2]_{\phi=0}$ and $[(R+1)/2]_{\phi=\pi}$ as shown in Figure 4. Thus, separation is: $S = C_{\max} - C_{\min}$. Maximum separation means an optimal coupling between the thermodiffusion and convection. According to the reference variable adopted for the mass fraction, separation is always greater than 1.

The comparison of numerical and analytical stream function, separation and temperature results is illustrated in Table 1 and Figure 5. Upon inspection of Table 1 it is observed that the comparison of temperature behavior is globally in good agreement. It is also noted a good agreement for the values of Nusselt number for a wide range of Ra, the maximum deviation was within one percent.

While a slight difference not more than 6% between analytical and numerical results of the stream function values is observed. We noted that the stream function vanishes on the walls ($r = 1$ and $r = R = 35/32$), this is due to the condition of adhesion to the surface; then it present an extremum for $r = 1.06$ (–0.123814 and –0.127929 for numerical and analytical results, respectively).

For the Separation the maximum deviation increases with the Rayleigh number. Analytical values for the separation are slightly lower than that calculated numerically. The results are very close at low Ra number, the maximum deviation increases with Ra (i.e. the error passes from 0.1% for $Ra = 0.1$ to 5.4% for $Ra = 0.5$).

The various results presented allow us to conclude that the analytical perturbation method developed till second order is more appropriate for small values of Ra.

In the following, to better understand the considered phenomenon it is instructive to study the effects of several parameters on the separation "S". The invoked parameters are the Rayleigh and Lewis numbers with the annulus dimension.

Table 2 highlights the evolving separation within the porous annular space according to Ra for three main values of the separation factor (sp). These values are: $sp =$ 0.1305; 0.12 and 0.1. Results indicate that the separation factor sp does not entail any significant change in the separation (S) for all Ra values. Subsequently, the value of sp will be set equal to 1.

In order to highlight the effect of Ra alone, both Lewis number, separation factor (sp) and gap ratio (R) were kept constant at values equal to 100, 0.1 and 35/32, respectively. Figure 6 shows the separation factor versus Ra in the range $Ra = 0$ to 50. A detailed investigation of the result show that the optimal separation is at $Ra = 1.75$. This maximum corresponds to the optimal coupling between convection and thermal diffusion. By raising Ra, the separation predictions show a gradual dip and then assume an asymptotic trend so that the effect of Ra on the separation seems to be insignificant. For slightly high Ra values, the flow is intense and it does not provide sufficient

Table 1. Comparison between analytical and numerical solution for $Le = 100$, $sp = 0.1$; and $R = 35/32$ for: Stream function ($Ra = 1$, $\phi = \pi/2$); mean Nusselt number (inner cylinder) and Separation.

Stream function ($Ra = 1$, $\varphi = \pi/2$)				Nusselt ($r = 1$)		Separation "S"	
r	Num. sol	Anal. sol	Ra	Num. sol	Analy. sol	Num. sol	Anal. Sol.
1.00			0.05	1.000000	1.000000001	0.957	0.957
1.01	–0.04817	–0.05026	0.1	1.000000	1.000000006	1.904	1.915
1.02	–0.08543	–0.08794	0.2	1.000000	1.000000561	3.738	3.831
1.03	–0.10994	–0.11329	0.3	1.000000	1.000000989	5.442	5.747
1.04	–0.12116	–0.12654	0.4	1.000000	1.000001520	7.259	7.663
1.05	–0.12381	–0.12792	0.5	1.000000	1.000002018	8.312	9.579
1.06	–0.11071	–0.11768	1.	1.000000	1.000004379		
1.07	–0.09238	–0.09601	10	1.000002	1.000072115		
1.08	–0.06119	–0.06313	20	1.000011	1.000287791		
1.09	–0.01881	–0.01925	30	1.000023	1.000649663		
1.0937			40	1.000047	1.001148666		

Table 2. Separation for $Le = 204$ and $R = 2^{(1/2)}$.

Ra	0.1	0.3	0.75	1	1.75	2	4	10	20
Separation for $sp = 0.1305$	3.092	3.335	2.250	1.903	1.597	1.224	0.790	0.462	0.309
Separation for $sp = 0.1$	3.064	3.336	2.251	1.903	1.334	1.222	0.788	0.461	0.308

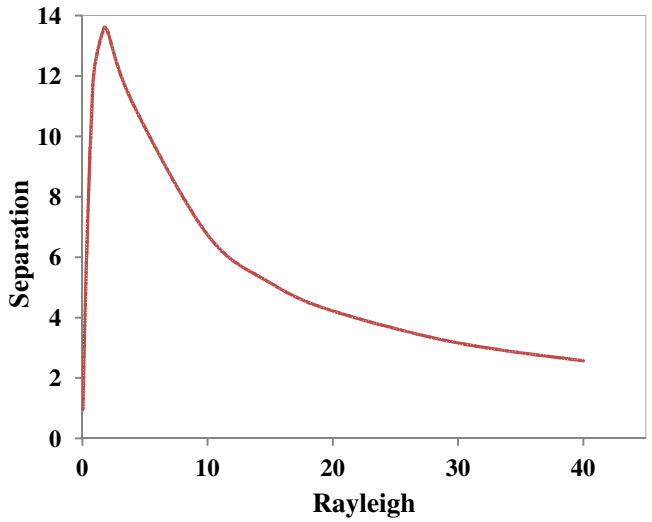

Fig. 6. Effect of Rayleigh number on separation curves for $Le = 100$, $sp = 0.1$ and $R = 35/32$.

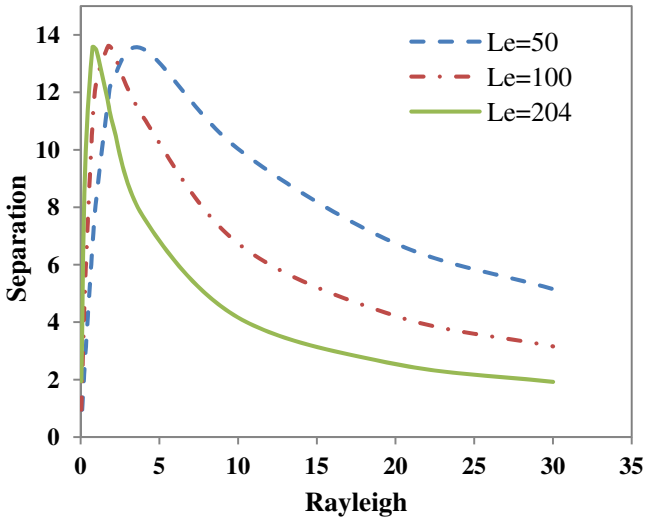

Fig. 7. Effect of Lewis number on separation curves for $sp = 0.1$ and $R = 35/32$.

separation. In contrast, for low Ra numbers, convection is smaller compared with the thermal-diffusion which controls separation time.

Furthermore, numerical calculations have been performed for different Lewis numbers. This number provides a measure of thermal diffusivity of a fluid to its mass diffusivity. Thus when Lewis number equals one, the thermal diffusivity equals to the mass diffusivity. This means that heat and species diffuse with the same characteristic time and the isothermal lines are congruent with the isoconcentration lines. Lewis number in the ongoing investigation was varied in the range from 0 to 100 as depicted in Figure 7 showing separation versus Ra.

Results shown in this figure indicate that the maximum separation value is practically independent on the Lewis number. Furthermore, the results also point out direct impact of Lewis number on the optimum Ra; they are inversely proportional. In fact, the optimal Rayleigh is even small when Lewis number increases (i.e : $Ra_{\text{opt}} = 1.75$; 3.75 for $Le = 100$ and 50, respectively).

To highlight the effects caused by changing the radius ratio (R) on the Separation, Figure 8 depict the separation following different annulus dimension and three aspect ratios; $R = 35/32$ (narrow gap), R and $R = 2^{1/2}$ (wide gap). The ratio (R) characterizing the annulus dimension is defined as a ratio between the outer and the inner radii of the crown ($R = r_e/r_i$). As can be seen, the ratio R has an influence on both the maximum separation and the optimum Rayleigh number. Indeed, reducing the dimensionless ratio (R), improve both the

Table 3. Effect of the gap width and mean radius on the separation ($Le = 100$, $sp = 0.1$).

$R = 1.09375$					$e = 3$					
r_e	r_i	E	Ra_{opt}	S	r_e	r_i	e'	R	Ra_{opt}	S
35	32	3	1.750	13.609	35	32	33.5	1.09375	1.75	13.609
70	64	6	1.000	13.595	40	37	38.5	1.08108	2.00	15.644
105	96	9	0.600	13.598	50	47	48.5	1.06382	2.75	19.506
140	128	12	0.500	13.500	55	52	53.5	1.05769	2.77	21.741
					60	57	58.5	1.05263	3.00	23.793
					70	67	68.5	1.04477	4.00	27.718
					102	99	100.5	1.03030	6.00	40.618

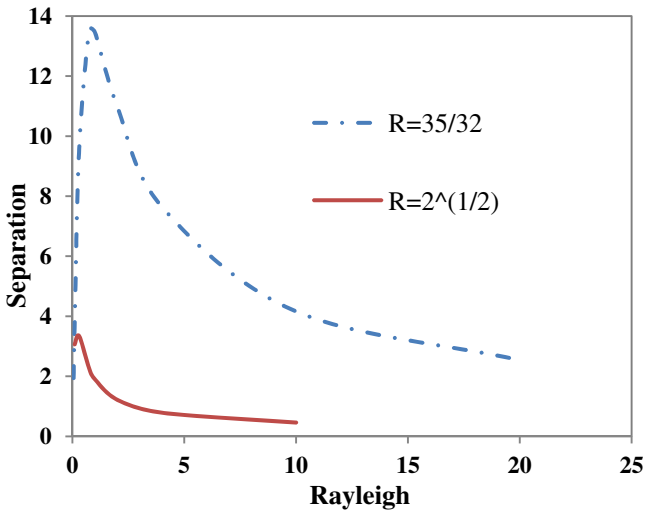

Fig. 8. Separation curves for $R = 2^{1/2}, R = 35/32$, $Le = 4$ and $sp = 0.1$.

maximal separation (S_{max}) and Ra_{opt} (i.e. $R = 35/32$: $Ra_{opt} = 1.75$ and $S_{max} = 13.75$; $R = 2^{1/2}$: $Ra_{opt} = 0.7$ and $S_{max} = 3$). The evolution of S also shows a rapid tendency toward an asymptotic behavior as Ra grows (i.e. $R = 2^{1/2}$: $Ra_{asym} = 10$ and $S_{asym} = 0.45$; $R = 35/32$: $Ra_{asym} = 30$ and $S_{asym} = 2$).

To achieve the effect of dimensionless parameter on the separation we focused on the influence of the crown section characterized by the gap width $e = (r_e - r_i)$. The dependence of the separation on the gap (e) is displayed in Table 2 showing the optimal separation for $Le = 100$, $sp = 0.1$ and $R = 1.09375$. Note that the annular space width (e) vary in multiples of the lowest value ($e = 3$) corresponding to $r_e = 35$ and $r_i = 32$. It follows that the optimal separation remains substantially constant around 13.5 regardless of the gap width e. In contrast, the optimal Rayleigh (Ra_{opt}) decreases when increasing diameters, therefore the gap (e).

In the general formalism the radii ratio is involved, in reality separation also depends on other quantities (dimension). Therefore, it is interesting to consider the same thickness (e) case and vary the mean radius of the crown; $e' = (r_e + r_i)/2$, just like R. Thus; Table 3 also illustrates separation (S) according to the average radius. The increase in the prediction separation is vivid as (e') is increased; this is due to the behavior of the mixture inside the cell. Increasing the mean radius will raise the workspace with considerable concentration distribution at the vicinity of the outer cylinder leading to a migration of the heavier component to the coldest side by simple diffusion. This component will be advected to the left side of the cell by convection so that the accumulation of the concentration difference between the top and bottom of the cell concentration creates great separation. In contrast to the previous case, the prediction of the optimal Rayleigh shows a growth as (e') increases.

5 Conclusion

This paper focuses on the characterization of binary fluid separation process in annular porous layer A horizontal annular cell is used instead of the rectangular cell, hence the novelty of this technique.

In a first part, an analytical resolution, of the coupled mass, energy and momentum equations, using the perturbation method was conducted. The development was performed till second order. Regarding the encouraging results obtained for temperature and stream function solutions, it was observed that for high values of the Rayleigh number (Ra above the optimal) concentration diverges (concentration varies proportionally with the Rayleigh number), although the value of Nusselt are in very good agreement with the numerical results.

In a second part, several numerical simulations, using the finite element method were performed to corroborate the results obtained analytically. These simulations allow a good agreement with the analytical temperature fields, the stream function and the separation parameter especially for Ra values less than the optimum.

Then, a parametric study based on the Rayleigh number Lewis number, separation factor porosity and characteristic size of the annular configuration was performed. It shown that for low ratios of R, the separation is optimal and varies proportionally with the increase of the mean radius.

Further experimental works are required as perspective to check the real functionality of the proposed annular geometry.

References

[1] K. Clusius, G. Dickel, Neues Verfahren zur Gasenmischung und Isotroprennung, Naturwisse 6 (1938) 546

[2] W.H. Furry, R.C. Jones, L. Onsager, On the theory of isotope separation by thermal diffusion, Phys. Rev. 55 (1939) 1083–1095

[3] S.R. De Groot, Théorie Phénoménologique du procédé thermogravitationnel de séparation dans un liquide, Physica 8 (1942) 801–816

[4] M. Lorenz, A.H. Emery, The packed thermal diffusion column, Chem. Eng. Sci. 11 (1959) 16–23

[5] J.P. Caltagirone, Thermoconvective instabilities in a porous medium bounded by two concentric horizontal cylinders, J. Fluid Mech. 76 (1976) 337–362

[6] P.J. Burns, C.L. Yien, Natural convection in porous medium bounded by concentric spheres and horizontal cylinders, Int. J. Heat Mass Transfer 22 (1979) 929–939

[7] H.H. Bau, Thermal Convection in a horizontal eccentric annulus containing a saturated porous medium: an extended perturbation expansion, Int. J. Heat Mass Transfer 27 (1984) 2277–2287

[8] K. Himasekhar, H.H. Bau, Two-dimensional bifurcation phenomena in thermal convection in horizontal concentric annuli containing saturated porous media, J. Fluid Mech. 187 (1988) 267–300

[9] M.P. Dyko, K. Vafai, A.K. Mojtabi, A numerical and experimental investigation of stability of natural convective flows within a horizontal annulus, J. Fluid Mech. 381 (1999) 27–61

[10] G. Desrayaud, A. Fichera, M. Marcoux, A. Pagano, An analytical solution for the stationary behavior of binary mixtures and pure fluids in a horizontal annular cavity, Int. J. Heat Mass Transfer 49 (2006) 3253–3263

[11] A.K. Mojtabi, S. Bories, M. Prat, and M. Quintard, Transferts de chaleur dans les milieux poreux, Techniques de l'Ingénieur, 2008, Available at: http://www.techniques-ingenieur.fr/base-documentaire/energies-th4/transferts-thermiques-42214210/transferts-de-chaleur-dans-les-milieux-poreux-be8250/

[12] N. Hadidi, Y. Ould-Amer, R. Bennacer, Bi-layered and inclined porous collector: Optimum heat and mass transfer, Energy 51 (2013) 422–430

[13] A. Khouzam, A. Mojtabi, M.-C. Charrier-Mojtabi, B. Ouattara, Species separation of a binary mixture in the presence of mixed convection, Int. J. Thermal Sci. 73 (2013) 18–27

[14] B. Elhajjar, A. Mojtabi, P. Costesèque, M.-C. Charrier-Mojtabi, Separation in an inclined porous thermogravitational cell, Int. J. Heat Mass Transfer 53 (2010) 4844–4851

[15] F. Oueslati, R. Bennacer, M. El Ganaoui, Analytical and numerical solution to the convection problem in a shallow cavity filled with two immiscible superposed fluids, Int. J. Thermal Sci. 90 (2015) 303–310

[16] FEMLAB AG, Comsol 33 Multiphysics FEM Software package, 2007